Journal of New Technology and Materials
JNTM
Vol. 04, N°01 (2014)106-111

OEB Univ. Publish. Co.

Optical and Structural Characterization of Fluorine-Doped SnO_2 Thin Films Prepared by Spray Ultrasonic

Soumaia Abbas[*1,2], Atman Ben Haoua[1,2], Boubaker Ben Haoua[2] And Achour Rahal[2,3]

[1]*Faculty of Mathematics & Materials Sciences, Univ Ouargla, 30000, Algeria.*
[2]*Laboratory VTRs, Univ El Oued, 39000, Algeria.*
[3] *Material Laboratory Department, Faculty of Sciences, Univ Biskra 07000,Algeria.*
Email*: abbes_soumia@yahoo.fr

Received: 30 April 2014, accepted 26 May 2014

Abstract

In this work, Fluorine-doped tin dioxide (FTO) films were prepared with spray ultrasonic technique using $SnCl_2$ and NH_4F as sources of SnO_2 and fluorine dopant, the films were deposited on MICROSCOPE SLIDES (REF 217102) used as glass substrates. The optical and structural properties of the films for different doping concentration (for 3-18 wt% NH_4F) were studied. The optical properties of the films were studied by UV–vis spectroscopy. Optical transmittance spectra of the films showed high transparency of about 72.8–83.5% in visible region which increases with increases F-doping. The optical gap for F-doped SnO_2 films was found in the range from 4.31 to 4.37 eV. The structure and topography of the ultra sonic deposited films were characterized by X-ray diffraction (XRD) and scanning electron microscopy (SEM). X-ray diffraction studies showed that the SnO_2: F films were polycrystalline and have preferential orientations along (2 0 0) planes and grain sizes in the range of 14–30 nm. SEM studies reveal the same observation on the effect of the fluorine doping.

Keywords: Spray Ultrasonic, FTO, UV-Visible Spectroscopy, X-ray diffraction (XRD);

1. Introduction

Transparent conductive oxides (TCO) are interesting materials in several applications, their important properties both electrical conductivity and transparency in the visible region, make them ideal candidates for optoelectronics, photovoltaic and catalytic applications. Among the different transparent conductive oxides, SnO_2 films doped with fluorine seem to be the most appropriate for use in many applications, owing to its low electrical resistivity and high optical transmittance. Non-toxicity and abundance of its components on Earth make it an ideal candidate for applications listed above. SnO_2 is available materiel and easy to deposit in thin films by using Ultrasonic Spray technique [1, 2]. Thin films of SnO_2 can be prepared by many techniques, such as chemical vapor deposition [3], sol-gel [4], pulsed laser deposition [5] and spray pyrolysis [6]. Among these techniques, new Ultrasonic Spray method is the most convenient technique because it is simple, low cost, easy to add doping materials and promising for high rate and mass production capability of uniform large area coatings in industrial applications [1, 2]. However, the preparation method affects on thin film structural properties, which play an important role in the optical and electrical properties of the film material. Doping with fluorine (F), antimony (Sb), cobalt (Co), Cerium (Ce), iron (Fe), palladium (Pd), niobium (Nb), molybdenum (Mo) and indium (In) has been achieved to improve tin oxide (SnO_2) property [7-13]. Among these dopants, fluorine has been shown to be the most effective and achieved commercial use due to its low cost and simplicity. A survey of literature reveals that most research works focus on the fluorine doped SnO_2 films used ammonium fluoride (NH_4F) as a fluorine precursor.

In the present work, SnO_2: F thin films were prepared by Ultrasonic spray technique on glass substrates using $SnCl_2$ and NH_4F as sources of SnO_2 and fluorine dopant. The aim of this work is to study the effect of the doping levels on some physical properties of SnO_2: F thin films such as optical transmittance, crystal structure and surface morphology. The results obtained are compared and discussed with the specified results by several researchers.

2. Results and discussion

2.1. Optical properties

Fig.1 shows UV–Vis transmittance spectra of F-doped SnO_2 thin films with various fluorine concentrations. The transmittance of all samples was more than 70% in the whole visible-light region (400 to 800nm), this transmittance value of fluorine doped tin oxide films are in good agreement with [14, 15]. The films doped with fluorine show increase in transmittance with increasing fluorine concentration, transmittance values are 72.8%, 76.2% and 83.5%, respectively for 6 wt. % F, 9 wt. % and 15 wt. % F. The increase in transmittance is attributed to the well-crystallized films [16]. A slight decrease in the optical transmittance at 18 wt. % (T= 76.8%) could be attributed to an excess free electrons in the films [17].

The comparison of transmittance, absorbance and reflectance of fluorine doped SnO_2 thin film (6 wt. %) is shown in Fig. 2.

Fig.3 shows the optical band gap E_g of SnO_2: F thin films. E_g can be deduced from transmission measurements using Tauc's relation Eq. 1[18]:

$$(\alpha h\upsilon)^2 = A(h\upsilon - E_g) \quad (1)$$

Where $h\upsilon$ is the photon energy, E_g is the optical band gap, A is a constant which does not depend on $h\upsilon$. E_g values calculated from the optical transmission were in the range of 4.31~4.37 eV (Table 1). The optical band gap values are higher than the value of E_g = 3.57 eV reported for single crystal SnO_2 [19] and are comparable to the value of E_g = 4.3 eV reported for F: SnO_x films [20-23]. This increase in band gap can be attributed to an increase in carrier concentration of the films due to F doping. Similar optical band gap values were reported for the SnO_2: F films [20, 21] The optical band gap decreases from 4.37 eV at 6 wt. % F to 4.31 eV at 15 wt. % with increasing fluorine concentration then it increases to 4.35 eV with 18 wt. % F doping.

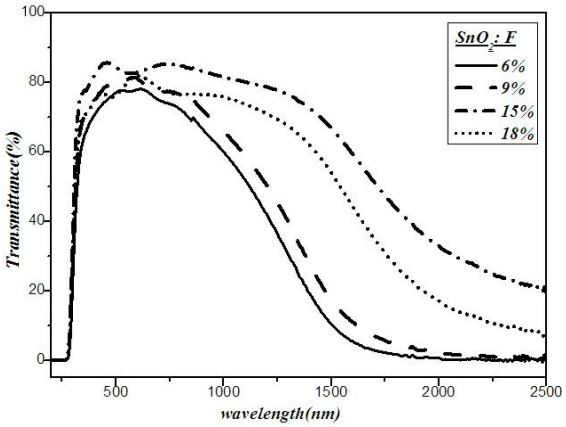

Figure 1: Transmittance spectra of SnO_2: F thin films as a function of Wavelength for different fluorine doping concentration (wt. %).

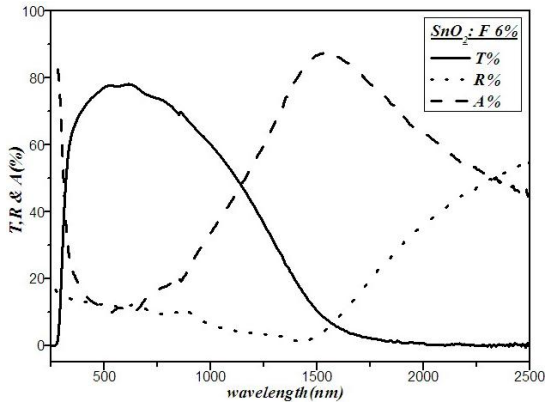

Figure 2: Transmittance, Reflectance and Absorbance spectra of F-doped SnO_2 thin film (6 wt. %)

The thickness of the film t is calculated from transmittance spectra using the following relation Eq. 2 [24, 25]:

$$t = \frac{\lambda_1 \lambda_2}{2(n_1\lambda_2 - n_2\lambda_1)} \quad (2)$$

Where n_1 and n_2 are the refractive indexes at the two adjacent maxima (or minima) at λ_1 and λ_2. The thickness of the films was determined to be between 365 nm and 712 nm; results are listed in Table 1 [26].

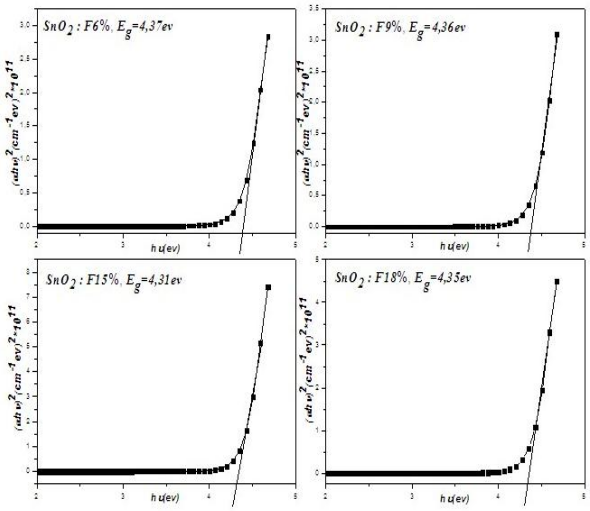

Figure 3: Optical band gap calculations of SnO_2: F thin films for different fluorine doping concentration (wt. %).

Table 1: Films thickness and optical gap values of SnO_2: F thin films for different fluorine doping concentration (wt. %).

F-doping wt. %	6 wt. %	9 wt. %	15 wt. %	18 wt. %
Films thickness (nm)	712.75	639	365.5	489.16
E_g (eV)	4.28	4.37	4.33	4.33

2.2. Structural analysis

The X-ray diffraction patterns of the SnO_2 films deposited by ultrasonic spry with different fluorine concentrations are shown in Fig. 4. For all deposited films, major peaks corresponding to the tetragonal SnO_2 (JCPDS No. 41-1445) were observed. It can be seen that all the films are polycrystalline and contain SnO_2 Tetragonal structure ($P4_2/mnm$ (136)), and no phase corresponded to fluorine was observed.

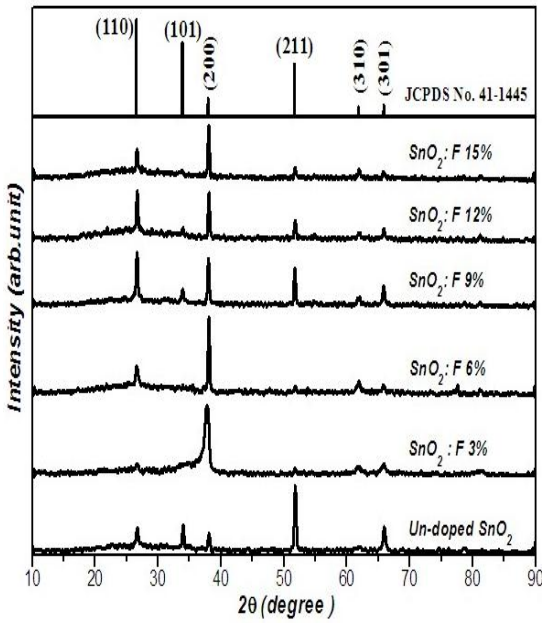

Figure 4: XRD patterns of F-doped SnO_2 films for different fluorine doping concentration.

The XRD results of SnO_2:F thin films prepared by Ultrasonic Spray exhibited five peaks at 2θ equal to 26.58°, 33.86°, 38.12°,51.85° and 66.,according to the (110), (101), (200), (211) and (301) planes, respectively. It is perceptible from the figure that the un-doped SnO_2 films grow along the preferred orientation of (2 1 1). The intensity of the plane (2 0 0) found increased with increasing fluorine doping concentration. In addition, after fluorine doping the peaks shift slightly to the less value of the Bragg angle [27]. In order to evaluate the preferred orientation of the SnO_2: F films, the texture coefficient T_{hkl} can be calculated from Eq. 3 [28]:

$$T_{hkl} = \frac{I_{hkl} / I_{0hkl}}{\frac{1}{N}\sum_{M} I_{hkl} / I_{0hkl}} \quad (3)$$

Where T_{hkl} is the texture coefficient of the plane (h k l), I_{hkl} is the measured intensity, I_{0hkl} is the corresponding standard intensity given in the ASTM cards (No. 41-1445), and N is the number of reflections. If the film had no preferred orientation, presumably the T_{hkl} would be one for all peaks. If the value of T_{hkl} is larger, the films may possess the (h k l) preferred orientation. The texture coefficients T_{hkl} of the films are listed in Table 2. It is indicated that all the SnO_2 films doped with 3, 6 and 15 wt. % F exhibit a preferred orientation with (200) plane whereas films doped with 9 and 12 wt. % F had no preferred orientation [29].

Table 2: Texture coefficients of SnO_2: F thin films for different fluorine doping concentration (wt. %).

	I_{110}	I_{101}	I_{200}	I_{211}	I_{301}	T_{hkl}
ASTM	100	75	21	57	15	-
Un-doped	27	30	21	69	28	1.27
3 wt. %	13	/	72	9	14	3.11
6 wt. %	31	/	80	11	12	3.14
9 wt. %	57	20	51	41	23	0.53
12 wt. %	53	16	51	23	15	0.58
15 wt. %	33	12	57	15	11	3.13

The crystalline sizes of SnO_2: F films given in the Table 3 are calculated according to the Scherrer's formula Eq. 4 [30]:

$$D = \frac{0.9\lambda}{\beta \cos\theta_{\beta}} \quad (4)$$

Where D is the crystallite size, β is the full width at half-maximum (FWHM) of the most intense diffraction peak, λ is the X-ray wavelength (1.5404 A°) and θ_{β} is the Bragg angle. A broad size distribution of about 27.53 nm was found for the un-doped film. However, for doped film at 9 wt. % Scherrer's equation applied to the most intense (1 1 0), (2 0 0) and (2 1 1) diffraction lines. A broad size distribution ranging from 27.28 nm to 30.35 nm whereas for doped films at 12 wt. % the average crystalline size calculated to (1 1 0) and (2 0 0) diffraction lines it ranging from 26.96nm to 29.45nm. In addition, the calculated sizes were in the range of 14 nm, 28.56 nm and 26.82 nm for 3 wt. %, 6 wt. % and 15 wt. %, respectively.

The lattice constants a and c, for the tetragonal phase structure is determined from XDR results using Eq. 5 [30]:

$$\frac{1}{d_{hkl}^2} = \frac{h^2 + k^2}{a^2} + \frac{l^2}{c^2} \quad (5)$$

Where d_{hkl} is the inter-planar distance, (h k l) are the Miller indices and a and c are the lattice constants. The calculated lattice constants a and c are given in Table 3. All the values were marginally larger than those of the standard SnO_2 with tetragonal structure in JCPDS card, which was caused by the F^- (substitution) of O^{2-} [26, 27].

Table 3: XRD analysis results of F-doped SnO_2 films for different fluorine doping concentration.

F-doping wt. %	Grain size D (nm)	Lattice Parameter a (A°)	Lattice Parameter c (A°)
Un-doped film	27.53	4.725	3.184
3 wt. %	14.03	4.763	3.141
6 wt. %	28.56	4.708	3.322
9 wt. %	27.28–30.35	4.725	3.184
12 wt. %	26.69–29.45	4.725	3.184
15 wt. %	26.289	4.742	3.200

The surface morphology of F: SnO_2 thin films deposited on glass substrate by ultrasonic spray for different fluorine doping concentration (3 wt. %; 6 wt. % and 12 wt. %), is shown in Fig. 5.

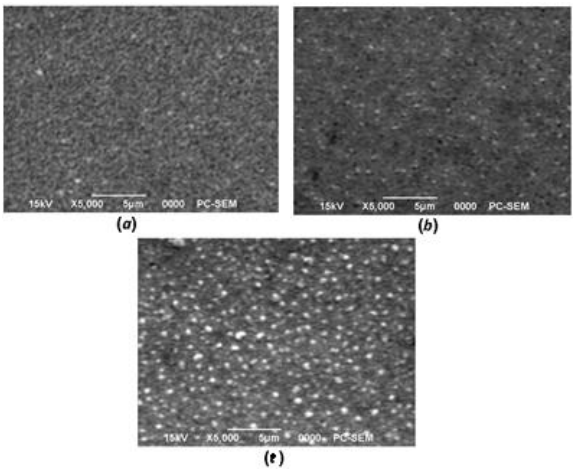

Figure 5: SEM micrographs of SnO_2: F films for various F-content (wt. % in film): (a) 3 wt. %, (b) 6 wt. %, and (c) 12 wt. %.

SEM micrographs show polycrystalline SnO_2 thin films with homogeneous distribution. From the SEM image, it is seen that the substrate is well covered with large number of fine grains and film surface is uniform. The films are continuous and consists inter-granular regions appearing darker [20, 29].

3. Conclusions

Thin films of fluorine doped tin oxide SnO_2 were successfully prepared on glass substrates by Ultrasonic spray technique. The effects of doping levels on the optical and structural properties of SnO_2: F thin films were experimentally investigated. The optical transmittance of the films found increased with increasing fluorine doping concentrations. The average visible transmittance of all samples was more than 70% in the visible region with an optical band gap of about 4.37-4.31 eV and thickness between 365 nm and 712 nm. X-ray diffraction studies revealed that all the films are polycrystalline with tetragonal structure. The preferred orientation of SnO_2: F films was found varying on doping level variation. The films show a preferred orientation along (2 1 1) for un-doped film whereas the films doped with 3, 6 and 15 wt. % F exhibit a preferred orientation with (2 0 0) plane. The grain size *D* was also found in the range of 14–30 nm. The results showed that this technique is superior to the conventional technique for both improving the film thickness uniformity and film transparency. In addition, the obtained results suggest that the deposited films can be used as transparent electrodes in solar cells applications.

References

[1] A. Rahal, S.Benramache, and B.Benhaoua, Journal of Semiconductors 34(8)083002 (2013) 1-4.
[2] A. Rahal, S.Benramache, and B.Benhaoua, Journal of Semiconductors 34(9)083002 (2013) 1-5.
[3] J. Szuber, G. Czempik, R. Larciprete, B. Adamowicz, Sensors and Actuators B 70 (2000) 177–181.
[4] H. Köse, A.O. Aydin and H. Akbulut, Acta Physica Polonica A 121(2012) 227-229.
[5] Ch.J. Lee, J.H. Lee, J.J. Kim, J.Y. Lee and H.Y. Lee, Integrated Ferroelectrics 115 (2010) 34–40.
[6] K. Murakami, K. Nakajima, S. Kaneko, Thin Solid Films 515 (2007) 8632–8636.
[7] Ch.M. Wang, Ch.C. Huang, J.Ch. Kuo and J.L. Huang, Surface & Coatings Technology 231 (2013) 374–379.
[8] G. Korotcenkov, I. Boris, V. Brinzari, S.H. Han and B.K. Cho, Sensors and Actuators B 182 (2013) 112–124.
[9] Z. Jiang, Z. Guo, B. Sun, Y. Jia, M. Li and J. Liu, Sensors and Actuators B 145 (2010) 667–673.
[10] B. Zhu, Ch. Yin, Z. Zhang, Ch. Tao and Liu Yang, Sensors and Actuators B 178 (2013) 418–425.
[11] G. Turgut, E.F. Keskenler, S. Aydın, E. Sönmez ,S. Dogan, B. Düzgün and M. Ertugrul, Superlattices and Microstructures 56 (2013) 107–116.
[12] E. Zampiceni , E. Bontempi , G. Sberveglieri and L. E.Depero, Thin Solid Films 418 (2002) 16–20.
[13] L. Francioso, A. Forleo, S. Capone, M. Epifani, A. M. Taurino and P. Siciliano, Sensors and Actuators B 114 (2006) 646–655.
[14] S. Chaisitsak, Sensors 11 (2011) 7127-7140.

[15] E. Elangovan, K. Ramamurthi, Applied Surface Science 249 (2005) 183–196.
[16] D. Tatar and B. Düzgün, Indian Academy of Sciences 79 No 1 (2012) 137–150.
[17] H. Kim and H.H Park, Ceramics International 38S (2012) S609–S612.
[18] J. Tauc, The optical properties of solids, Éd. J. Tauc, New York: Academic Press (1966).
[19] R. Summit, J.A. Marley and N.F. Borrelli, J. Phys. Chem. Solids 25 (1964) 1465.
[20] A.A. Yadav, E.U. Masumdar, A.V. Moholkar, K.Y. Rajpure and C.H. Bhosale, Physica B 404 (2009) 1874–1877.
[21] H. Khallaf, Ch.T. Chen, L.B. Chang, O. Lupan, A. Dutta, H. Heinrich, F. Haque, E. del Barco and Lee Chow, Applied Surface Science 258 (2012) 6069–6074.
[22] Stjerna, E. Olsson, C.G. Granqvist, J. Appl. Phys. 38 (1967) 3767.
[23] H. Kim, R.C.Y. Auyeung and A. Pique, Thin Solid Films 516 (2008) 5052.
[24] J. C. Manifacier, M. De Murcia and J. P. Fillard, Thin Solid Films 41 (1977) 127-135.
[25] M. Jubault, Doctorate Thesis, University of Pierre and Marie Curie, France (2009).
[26] D.R. Acosta, E.P. Zironi, E. Montoya and W. Estrada, Thin Solid Films 288 (1996) 1-7.
[27] Q. Gao, Q. Liu, M. Li, X. Li, Y. Liu, Ch. Song, J. Wang, J. L. Ge Shen and G. Han, Thin Solid Films 544 (2013) 357–361.
[28] I. Yang, H. Zhao , Q. Chen, Sh. Liu, H. Sha and F. Zhang, Thin Solid Films 520 (2012) 5691–5694.
[29] A. Muthukumar, G. Giusti, M. Jouvert,V.Consonni and D. Bellet, Thin Solid Films 545 (2013) 302–309.
[30] S. Sujatha Lekshmy, G. P. Daniel and K. Joy, Applied Surface Science 274 (2013) 95–100.